Design and implementation of embedded sensors based on electrical resistivity to determine water content profiles in thick concrete structures

Joanna Badr, Yannick Fargier, Fabrice Deby, Géraldine Villain, Sérgio Palma Lopes, Sylvie Delepine-Lesoille, Jean-Paul Balayssac, Louis-Marie Cottineau

9th European Workshop on Structural Health Monitoring
July 10-13, 2018, Manchester, United Kingdom

Design and implementation of embedded sensors based on electrical resistivity to determine water content profiles in thick concrete structures

J. Badr[1, 2], Y. Fargier[2, 4], F. Deby[1], G. Villain[2], S. Palma-Lopes[2], S. Delepine-Lesoille[3], J.P. Balayssac[1], L.M. Cottineau[2]
1 Université Paul Sabatier III, Toulouse, France,
badr@insa-toulouse.fr, f_deby@insa-toulouse.fr, balayssa@insa-toulouse.fr
2 IFSTTAR, Sites de Nantes et de Bron, France,
joanna.badr@ifsttar.fr, yannick.fargier@ifsttar.fr, geraldine.villain@ifsttar.fr, sergio.lopes@ifsttar.fr, louis-marie.cottineau@ifsttar.fr
3 Andra, Paris, France,
sylvie.lesoille@andra.fr
4 CEREMA, Normandie-Centre, Site de Blois, France,
yannick.fargier@cerema.fr

Abstract

The French national radioactive waste management agency (Andra) aims to insure the durability of thick concrete structures used for waste repository. To this end, concrete water content is one of the main parameters governing the long-term durability of these structures, therefore an accurate estimation of its profile is important. This research focuses on an electrical resistivity technique, which is highly sensitive to the water content in concrete.
Our work aims to design a prototype of embedded sensors in concrete structures to measure the resistivity profile with depth and the water content profile after calibration. The study highlights the capability of different types of sensors to measure the resistivity profile of a 30cm-thick concrete section. Several numerical studies are conducted to design different possible configurations of the embedded sensors and to optimize the sensors geometry in order to obtain the most relevant configuration. Several types of sensors are tested on small specimens; for instance Wenner type (aligned and equidistant four-pin probe resistivity method), proved capable of identifying the resistivity profile. The methodology for observing, measuring and monitoring the resistivity profile over time is studied.

1. Introduction

Andra's mission is to manage the radioactive waste coming from the French nuclear industry for the short, medium and long term, in order to protect the current and future generations and their environment from the potential harmful effects of this waste (1). It is therefore a mission of sustainable development. The main idea is to contain the radioactive waste by storing it within a deep geological formation (Figure 1) (Cigeo project in Bure-France). These repository facilities will be subject to different environmental conditions throughout their lifespan. Indeed, some radioactive wastes are exothermic and cause the temperature to rise up to fifty degrees Celsius inside the repository cells (1). Thus, to limit the heating of the cementitious materials within the cells, a ventilation system will be implemented. However, the ventilation will cause the

surrounding concrete to dry, thereby generating a water content gradient that will cause changes in the long-term behaviour of the structures (1). Consequently, the main objective of this study is to design and produce a prototype of embedded sensors for the radioactive waste repository structures to monitor the water content profile. The desired resolution (as a function of the depth z in the concrete) for the Andra application is: several points in the concrete, ideally every 1 cm for the first centimetres, then a point every 5 cm in the middle.

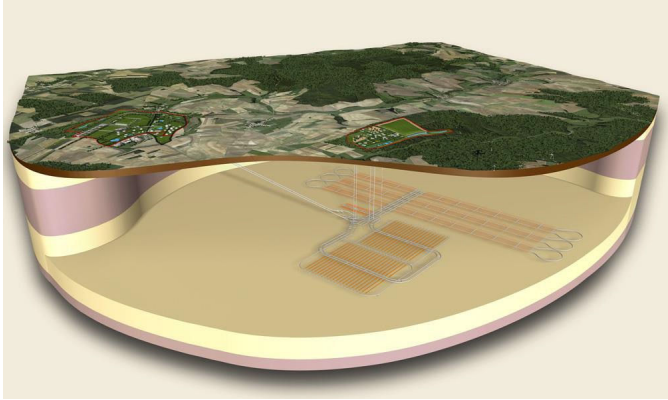

Figure 1. Schematic diagram of the surface and underground installations of the Cigeo Project (2).

Various non-destructive techniques are capable of characterizing the concrete water content such as capacitive probes (3), TDR (Time Domain Reflectometry) probes (4), GPR (Ground Penetrating Radar) (3) and electrical resistivity (3, 5-8) which is the method used in this study.

It was envisaged to work at the ½ scale (30cm thickness instead of 60cm planned for the Andra application) because the conditioning time to impose a water content gradient in a 60cm thick sample would be too long.

Therefore, this paper describes the development of an embedded device, based on electrical resistivity, to monitor the water content profile. The study focuses on the numerical modelling and validation in small concrete specimen as well.

2. Electrical resistivity

The electrical resistivity is a material property characterized by the mobility of the existing ions in the interstitial solution. It is therefore strongly influenced by the aqueous phase of the concrete. The higher the concrete porosity is, the higher the concrete liquid phase is and therefore the lower the concrete resistivity is. The relationship between the electrical resistivity and the concrete water content is studied in many works in literature (5-8).

Different versions of the 4-point electrode method have been used in near-surface geophysics, but for an application on the concrete, the Wenner configuration (8-13) is often used since it has a good signal-to-noise ratio and a good sensitivity to the resistivity's variations between the surface and the depth (14). For this configuration, the electrodes are arranged in line with a constant inter electrode spacing. The current is

injected on the external electrodes and the potential drop is measured on the internal electrodes.

The electrical resistivity is influenced by the homogeneity of the material and connected to the electrical resistance by a geometric factor G_R which depends on the geometry of the structure and on the shape and positions of the electrodes in the structure. In the case of a heterogeneous medium, an "apparent" resistivity ρ_a is measured, given by the following equation *(1)*:

$$\rho_a = G_R.R = G_R.\frac{\Delta V}{I} \qquad (1)$$

where ρ_a [Ω.m] is the apparent resistivity, G_R [m] is the geometric factor, ΔV [V] is the measured potential drop and I [A] is the intensity of the electric current injected.

In the case of some trivial geometries (e.g. a cylindrical sample, a half-space medium) there are analytical expressions for the geometric factors. In other cases, geometrical factors can be numerically determined, e.g. by a finite element (FE) calculation explained in detail in section 3.1.

To make an electrical resistivity measurement, it is possible to carry out either a surface measurement (or even a set of numerous measurements from which the resistivity can be evaluated at different depths by an inversion procedure (13)), or a measurement at depth using an embedded device. Different methods of surface electrical resistivity measurements are used. A multi-ring resistivity cell (8) for concrete sample evaluation and a multi-electrode surface resistivity probe for on-site applications (8, 13) are capable of identifying resistivity gradients over depth. However, the problem associated with these methods is that of achieving good electrical contact between the electrodes and the concrete. These methods are not optimal for monitoring, the estimation of the water content profile is indirect (loss of resolution in the middle).

3. Numerical modelling

The numerical simulation is conducted using a 3D electrostatic model and the AC/DC module integrated in the COMSOL Multiphysics®, a commercial software based on the finite element method. The purpose is to choose the best configuration to optimize the geometry of the multi-electrode device (number, shape and relative positions of the electrodes). We modelled a slab of 60cmx60cmx30cm inside which sensors of different geometries are placed using a very refined mesh (maximum dimension of the tetrahedral element is equal to 0.1cm). The shape and dimensions of the electrodes is studied in section 3.3. The boundary conditions are zero current flows on all boundaries to simulate a perfect insulation. The resistivity distribution is constant, to obtain the geometric factors G, and variable to study the profiles in depth.

3.1 Geometric factor modelling

The calculation of the geometric factors which is executed by definition on a homogeneous medium having the same geometry as the non-homogeneous medium that

is to be studied, and implementing the exact same electrode positions and combinations, is based on the approach proposed by Marescot (15):

$$G_R = \rho_0 . \frac{I_0}{\Delta V_0} \quad (2)$$

where ρ_0, ΔV_0 and I_0 are respectively the apparent resistivity, the measured potential drop and the intensity of the electric current injected in the homogeneous medium.
By defining a current I_0 = 1A and a resistivity ρ_0 = 1 Ω.m we symbolically obtain:

$$G_R = \frac{1}{\Delta V_0} \quad (3)$$

Thus, for each electrode configuration, a reference potential drop ΔV_0 is calculated from the finite element model and the corresponding geometrical factor is obtained.

3.2 Imposed resistivity profile with depth

We use Weibull-type resistivity profile which is a function that can match realistic water content profiles in concrete (6).

The general form of the Weibull distribution function is given in equation *(4)*:

$$F(z, k_w, \lambda, \rho_{max}, \rho_{min}) = (\rho_{max} - \rho_{min}) * e^{-(\frac{z}{\lambda})^{k_w}} + \rho_{min} \quad (4)$$

This function has 4 parameters: k_w the shape parameter, λ the scale parameter and the two parameters ρ_{min} and ρ_{max} which modify the minimum and maximum of the function. At this stage of the study, having no initial information on the resistivity profile, the parameters ρ_{min} and ρ_{max} are determined based on the range of electrical resistivity for different types of concrete (10). For a CEM I Ordinary Portland Cement, the resistivity varies between 50 and 200 Ω.m in humid conditions, and between 100 and 400 Ω.m under natural conditions without carbonation. Thus, the parameters ρ_{min} and ρ_{max} chosen in the numerical simulation are respectively 50 Ω.m and 400 Ω.m. The shape and scale parameters k_w = 3 and λ = 1/13 m^{-1} are determined to have a progressive decrease in the resistivity as a function of the depth z (Figure 2). Thus the equation of the resistivity variation imposed in the numerical model is given in equation *(5)*:

$$\rho\,(z) = 350 * e^{(-13*z)^3} + 50 \quad (5)$$

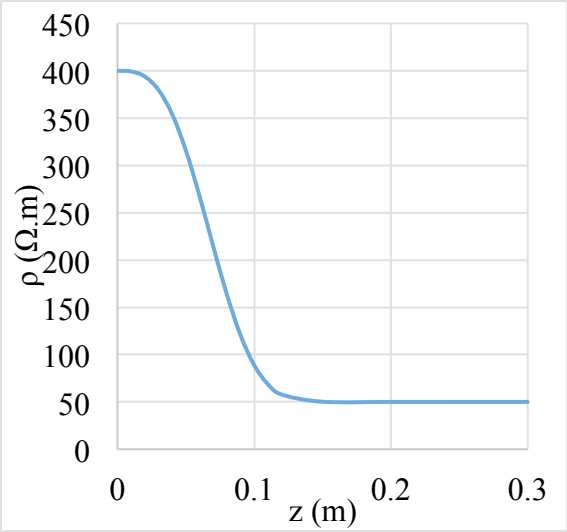

Figure 2. Weibull type of electrical resistivity profile as a function of depth in the numerical model

3.3 The Wenner configuration

The Wenner configuration consisting of four electrodes separated from each other by a distance a = 1cm, is placed at a given depth z and aligned parallel to the surface and therefore perpendicular to the direction of the resistivity gradient to be determined. Seven Wenner sensors are modeled at depths z = 1cm, 2cm, 3cm, 4cm, 5cm, 6cm and 10cm respectively in the numerical model (Figure 3). Several dimensions for the sensor geometry and different electrode shapes (point, cylindrical, spherical…) were studied. Two electrode shapes (point vs cylindrical) have been compared in section 3.4.1.

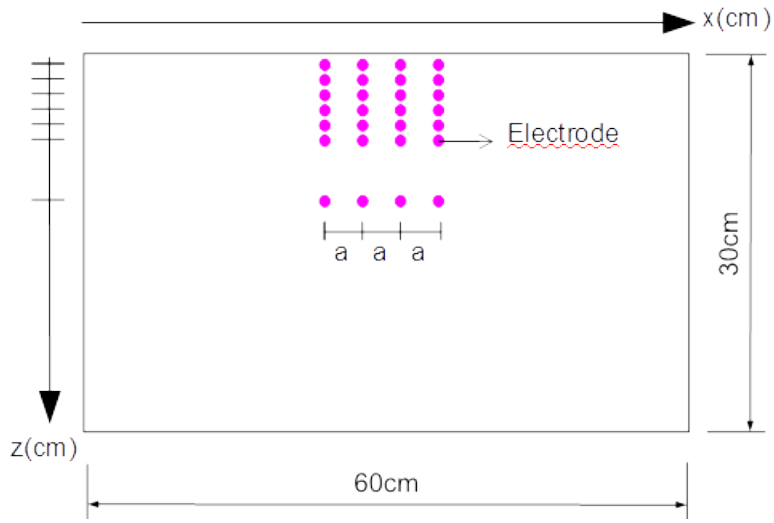

Figure 3. Schematic view of the slab section in the numerical model

3.3.1 Effect of the dimension of the electrodes

In order to compare the sensor's ability to match the imposed resistivity profile in the model *(equation 5)* and to show the influence of the electrodes dimensions on the sensor sensitivity (to know if we can simulate small cylinder electrodes by points or by their true size), we plotted the resistivity profile in Figure 4 as a function of depth for two

electrode dimensions: point (modelled by a point in COMSOL Multiphysics) and cylinder (modelled by a cylinder having a diameter of 0.3cm and a height of 0.3cm).

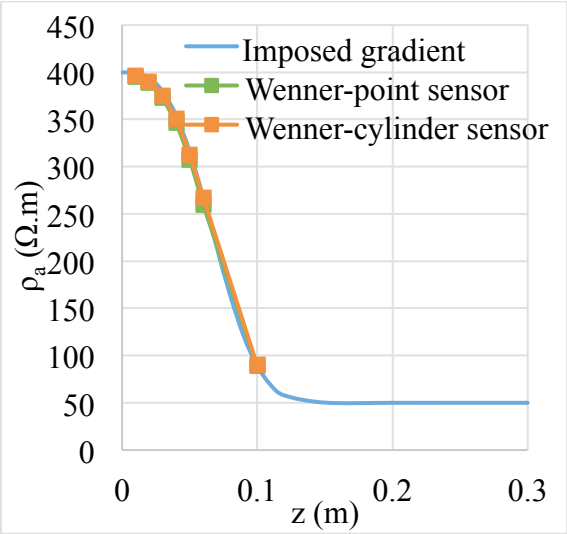

Figure 4. Simulated Wenner apparent resistivities for point and cylindrical electrodes compared to the imposed (actual) resistivity profile as a function of depth in the concrete slab

It is obvious from Figure 4 that the differences between the actual resistivity distribution (imposed profile with depth) and the simulated apparent resistivities are relatively small (around 1.7%). The difference between the two electrodes dimensions is 1% on average. Consequently, for the rest of our work, the point electrodes will be retained to overcome the problems of mesh at the cylindrical electrodes which have a small volume compared to the volume of the slab.

This result is encouraging and proves the capability of Wenner sensors having the size, orientation and positions above-mentioned to determine the electrical resistivity profile accurately.

3.3.2 Influence of the spacing between electrodes

This section highlights the influence of the spacing between the electrodes on the response of the sensor. Three different spacing measurements are considered: 1cm, 2cm and 5cm. It can be seen from Figure 5 that as the distance between the electrodes decreases, the difference between the apparent resistivities and the actual resistivity profile in the medium decreases. Indeed, Millard (16) recommended making the measurements with an electrode spacing small enough to get closer to the real resistivity value of the medium. Thus, for the rest of our work, a distance of 1cm will be retained.

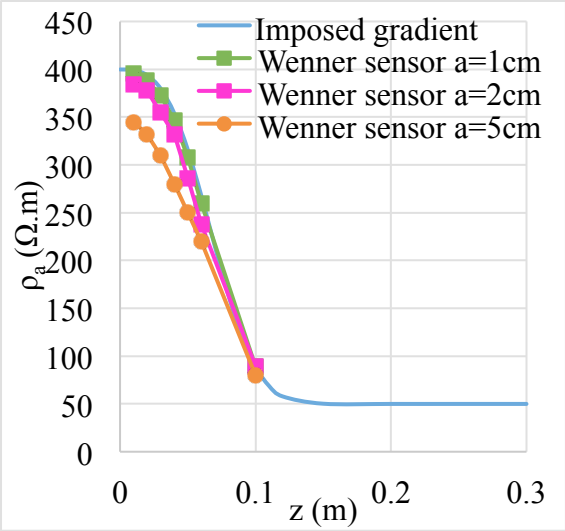

Figure 5. Wenner apparent resistivities for different inter-electrode spacing compared to the imposed (actual) resistivity profile as a function of depth in the concrete slab

4. Experimental campaign

To validate the numerical study, an experimental campaign was led on concrete specimen submitted to drying during 3 months.

4.1 Description of the Wenner sensor

Three plates in Bakelite (Figure 6 (a)) of dimensions 5cmx1cmx0.2cm were placed at different depths z = 2cm, 6cm and 10cm in a hollow PVC mould of inner dimensions 20cmx20cmx20cm. Each plate is perforated by 4 stainless pins aligned and separated from each other by a distance of 1cm.

A batch of concrete (cement type I) was then cast to fill up the cube. After 28 days of curing, the cube was sealed with aluminium foil on the sides and the underside faces; only the upper face was kept in contact with the air to ensure a unidirectional drying. We are thus close to the drying conditions of the full-scale elements. The cube was placed in a room at a constant temperature T = 20 ± 2 °C.

a) 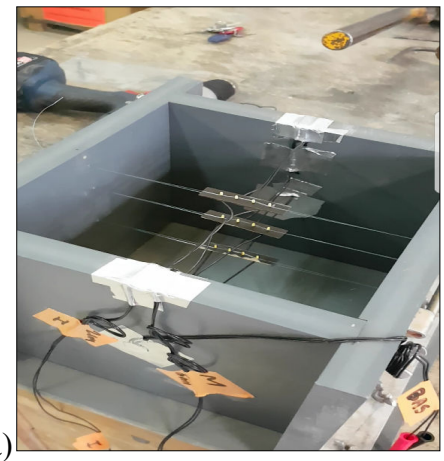 b) 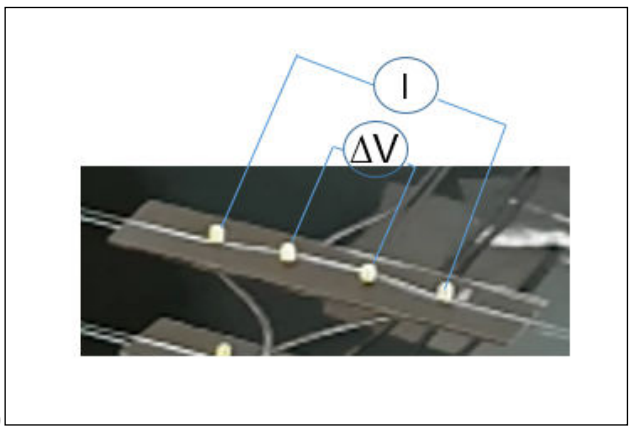

Figure 6. (a) Wenner arrays in the concrete block, (b) the measurement principle

The measurement principle is described in Figure 6 (b) where the current intensity I is injected on the two external electrodes and the potential drop (ΔV) is measured between the two internal electrodes. Therefore, we obtain 3 resistance measurements ΔV/I at different depths.

4.2 Results

A study showing the variability of the resistance as a function of the current intensity (Figure 7 (a)) is carried out showing a stable value of the resistance whatever the intensity of the injected current is: 0.5, 1 or 2 mA. The relative variation is in the range of 0.2% to 0.9% for each depth. In principle V is proportional to I, therefore this test verifies that we are in proximity of I where this linearity is verified. Another study showing the repeatability of the resistance measured over time (Figure 7 (b)) is carried out showing a stable resistance value during 12 hours on hardened concrete (after 28 days of curing) under saturated conditions (with t'0 marking the beginning of the acquisition). For a concrete specimen at the end of cure under saturated conditions, stable values of resistivity as a function of time are expected because the concrete does not evolve too much at this stage. The coefficient of variation varies between 0.7% and 1.3% during 12 hours.

a)

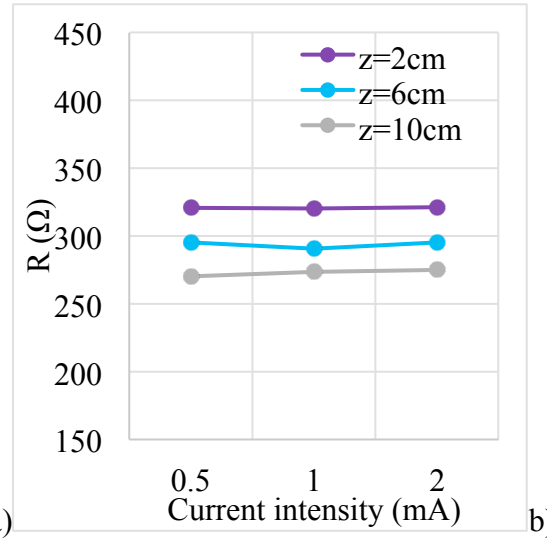

b)

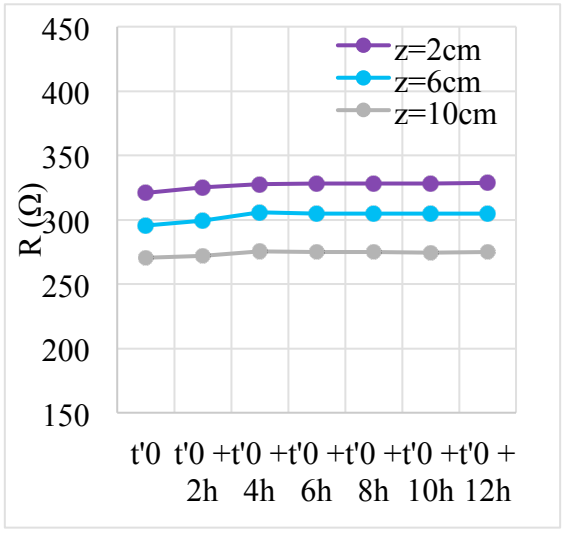

Figure 7. Stability of the Wenner measurements relative to (a) current intensity, (b) time under saturated conditions

The numerical modelling of the cube containing the Wenner arrays enables to calculate the geometric factors corresponding to each array at a given depth in order to calculate the apparent resistivity values from the measured resistances (*equation 1*). During the drying of the concrete, the change in the apparent resistivity profile as a function of time is illustrated in Figure 8 with t0 marking the beginning of drying process.

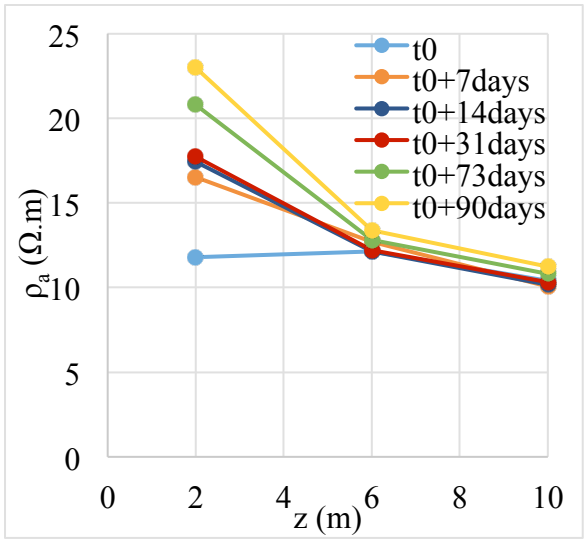

Figure 8. Variation of the Wenner apparent resistivity profile measured as a function of time

Figure 8 shows an increase in the apparent resistivity value over time revealing the evolution of the concrete due to the drying process. The water evaporates from the face in contact with the air creating a water content gradient between the two faces of the cube. It is noted on this graph that the apparent resistivity at z=2cm increases more rapidly over time than that at z=6cm and 10cm, the concrete being drier on the surface during this uni-directional drying.

The results for the Wenner arrays are therefore promising. However, the main disadvantage of this system, is the size of the electrical cables linked to the pins which could hinder the passage of the aggregates during concrete casting. In particular if the required gradient resolution is 1 cm, a great number of electrodes will be necessary, therefore a great number of cables would be required.

5. Conclusion

In this paper, a Wenner device was used in order to estimate the resistivity profile in concrete from the surface to the core. Several numerical studies were conducted, by changing the shape of the electrodes and the geometry of the sensors in order to obtain the most relevant configuration (i.e. the configuration that yields apparent resistivity as close as possible to the actual resistivity profile). Experimental measurements were carried out on a concrete cube at different times of drying. The apparent resistivity data are shown sensitive to the evolution of concrete drying over time. Calibration curves, transforming the resistivity profile into a saturation degree profile, are currently being studied.
In perspective, the Wenner sensor can be used in many structures to monitor the resistivity profile. However, such kind of sensor may not be adapted for a gradient resolution of 1cm.

Acknowledgements

The authors would like to thank Carole Soula in Université Paul Sabatier III, Toulouse for the technical support she provided.

References

1. Andra, Dossier "Argile-Synthèse-Evaluation de la faisabilité du stockage géologique en formation argileuse", Collection Les Rapports, 2005
2. Cagnon H., "Influence des variations thermo-hydro-mécaniques sur le comportement différé du béton" (Thesis), Université Toulouse 3, France, 2015.
3. Du Plooy R., Villain G., Palma Lopes S., Ihamouten A., Dérobert X., Thauvin B., "Electromagnetic non-destructive evaluation techniques for the monitoring of water and chloride ingress into concrete: a comparative study". Mater Struct; 48(1–2):369–86, 2015.
4. Yu, X.B., Liu, Y., "Development of Time Domain Reflectometry Instrument for QA/QC of Fresh and Early Stage Concrete", Civil Engineering Department, Case Western Reserve University, Cleveland, Ohio, 2010.
5. Lataste J-F., "Évaluation non destructive de l'état d'endommagement des ouvrages en béton armé par mesures de résistivité électrique" (Thesis), Bordeaux 1, France, 2002.
6. Fares M., Villain G., Thiery M., Derobert X., Palma Lopes S., "Estimation of water content gradient and concrete durability indicators using capacitive and electrical probes", In: International Symposium Non-Destructive Testing in Civil Engineering (NDT-CE), Berlin, Germany, 2015.
7. Villain G., Sbartaï Z.M., Lataste J-F., Garnier V., Dérobert X., Abraham O., Bonnet S., Balayssac J-P., Nguyen N.T. and Fares M., "Characterization of water gradients in concrete by complementary NDT methods", Berlin, Germany, 2015.
8. Du Plooy R., Palma Lopes S., Villain G. and Dérobert X., "Development of a multi-ring resistivity cell and multi-electrode resistivity probe for investigation of cover concrete condition", NDT & E International 54: 27–36, 2013.
9. Wenner F., "A method for measuring earth resistivity", Journal of the Washington Academy of Sciences 5 (16): 561–563, 1915.
10. Polder R., "Test methods for on-site measurement of resistivity of concrete - a RILEM TC-154 technical recommendation", Construction and Building Materials, Near Surface Testing of, 15 (2): 125‑31, 2001.
11. Andrade C., Polder R. and Basheer M., "Non-destructive methods to measure ion migration", RILEM TC, 91–112, 2007.
12. Liu Y., Suarez A. and Presuel-Moreno F.J., "Characterization of New and Old Concrete Structures Using Surface Resistivity Measurements", Page 263, 2010.
13. Fares M., "Evaluation de gradients de teneur en eau et en chlorures par méthodes électromagnétiques non-destructives", (Thesis), Université Nantes Angers Le Mans, France, 2015.
14. Dahlin T. and Zhou B., "A numerical comparison of 2D resistivity imaging with 10 electrode arrays", Geophysical prospecting 52 (5): 379–398, 2004.
15. Marescot L., Rigobert S., Palma Lopes S., Lagabrielle R. and Chapellier D., "A general approach for DC apparent resistivity evaluation on arbitrarily shaped 3D structures", Journal of Applied Geophysics 60 (1): 55–67, 2006.
16. Gowers K. and Millard S., "Measurement of concrete resistivity for assessment of corrosion", ACI Materials Journal 96 (5), 1999.